

TIME-RESOLVED X-RAY DIFFRACTION STUDIES ON BIOLOGICAL SYSTEMS

G. RAPP

EMBL c/o DESY, Notkestr. 82, W-2000 Hamburg 52, Germany

Understanding of biological function requires knowledge both on structural and dynamical aspects. The aim of time-resolved X-ray diffraction is to combine structural and kinetic methods by monitoring structural or conformational changes within a single protein or assemblies of proteins during their biological action in real time. This requires (i) a powerful X-ray source, (ii) appropriate detectors capable of dealing with high local and total count rates and (iii) a suitable trigger mechanism. These aspects are briefly discussed with emphasis on light as trigger for initiation of structural or conformational changes. Examples are presented on muscle contraction, lipid phase transitions, the photocycle of bacteriorhodopsin and the application of Laue crystallography on the protein p21.

PACS numbers: 61.10.-i, 87.80.+s, 52.50.Jm

1. Introduction

This lecture is intended to give a survey on applications of X-ray diffraction and scattering on biological systems. Since a huge amount of work is published in this area, we do not claim to cover this field completely and objectively. The intention is to discuss the general approach in this topic and to describe a selection of experiments carried out at the Hamburg outstation of the European Molecular Biology Laboratory (EMBL) in more detail. The interested reader will find further information on time-resolved studies with emphasis on integrating detectors in [1]. In Refs. [2, 3] applications of X-ray absorption, scattering and diffraction on biological samples are summarized. Similar, but more recent work is presented in Refs. [4-6].

Understanding of the function of biological systems requires knowledge both structural and kinetic aspects of macromolecular systems. Let us consider biological systems like muscle fibres or membranes. They consist of numerous macromolecular components whose interplay leads to its specific biological function. How do these systems work on a molecular level, i.e. how can a muscle with 1 cm² cross-section lift a weight of 2 kg or more? Or the membrane which is a barrier between two completely different environments and simultaneously has to provide

the channels for e.g. signal transmission or the exchange of matter. Investigation of these complex systems necessarily means to collect structural and functional information about the subunits involved, which then hopefully leads to a solution of the puzzle.

What do we mean by "time-resolved" experiments? Consider Fig. 1 where the time scales of some biological relevant processes are shown together with a selection of physical methods. It follows that time-resolved experiments could cover the

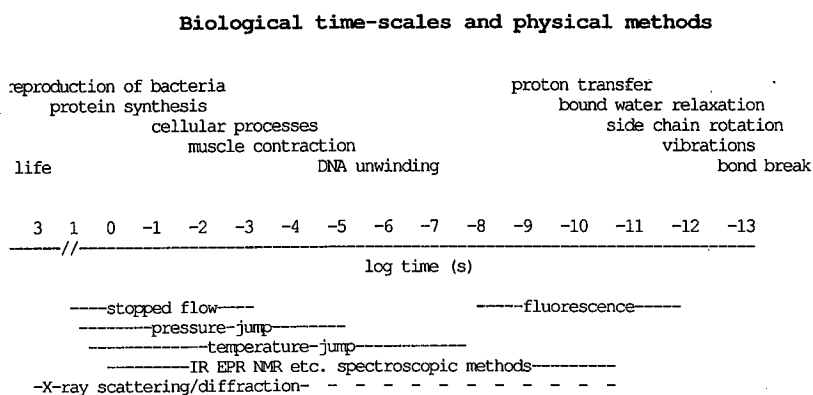


Fig. 1. Time scales of biological relevant processes and physical methods. X-ray diffraction experiments reach the μs range even though ps time resolution using the pulse structure of synchrotrons is possible.

range from hours to femtoseconds. With one exception (the Laue crystallographic approach on p21 as described below) we understand time-resolved experiments covering the sub-second range. The approach can be twofold. First, the scattered intensities or parts of them are monitored solely as a function of time, like e.g. a fluorescent signal. Second, both the temporal and spatial information of the overall diffraction pattern is recorded. Here time-resolved X-ray diffraction offers the great advantage of obtaining structural information together with the kinetics of its change. The technical difficulties arise from the need of (i) a powerful X-ray source, (ii) suitable detectors capable of dealing with the high local and total count rates and (iii) an appropriate trigger mechanism to initiate a reaction or a change.

The availability of the samples range from single crystals over semi-ordered fibrous aggregates to randomly distributed molecules in solution. By nature of the X-ray diffraction method, the better a sample is ordered the higher the spatial resolution. Often the samples are available only in solutions. Here the scattered intensities are solely a summation of the scattered intensities of the individual particles. One can measure changes (i) in the forward scattering resulting e.g. from polymerization, (ii) in the radius of gyration resulting e.g. from a change in shape and (iii) in the intensity distribution originating from partial orientation of the molecules (see [7]). General aspects of small-angle scattering are discussed in more detail in the lecture of Fratzl [8]. Experiments on X-ray scattering are reviewed in e.g. [7]. Here we restrict ourselves to diffraction experiments.

2. X-ray beamline

Synchrotron radiation and beamline instrumentation have been discussed in the lectures of Haensel, Kvick and Malgrange [9–11]. Therefore we summarize some relevant aspects of beamline requirements for biological samples. Since the questions behind the experiments on biological samples are so diverse as the samples themselves, there is no unique solution and any beamline is a trade-off between various requirements:

(a) About flux, brightness, and brilliance (see [10]). Since the samples vary in size from less than 100 μm to more than 1 mm, there is no unique answer to the question regarding a high flux, brightness, or brilliance source.

(b) Tunability would be advantageous for (i) adjusting the wavelength to the thickness of the sample and (ii) studying anomalous effects. The optimal thickness t of the sample scales with the linear absorption coefficient μ as $t = 1/\mu$.

(c) Clean source. Especially in small-angle scattering care has to be taken to reduce additional instrumental background created from optical elements, windows, and the gas in the X-ray beam. The samples are usually weak scatterers (scattering power 10^{-6} or less) and cannot be investigated in vacuum. As much as possible of the pathway of X-rays has to be evacuated and the necessary windows have to be selected carefully.

EMBL X 13

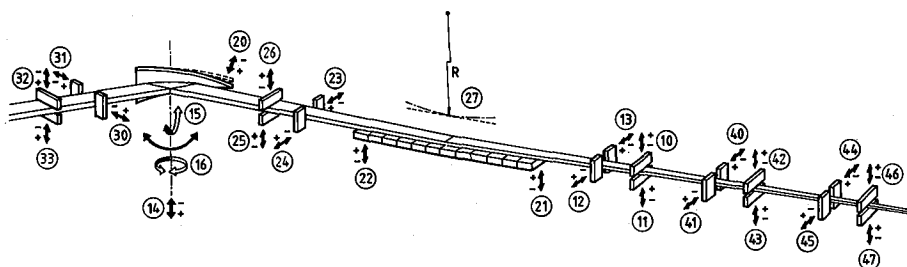


Fig. 2. Sketch of the EMBL beamline X13. The white beam falls on a bendable triangular monochromator. 12 plane quartz mirrors on a bendable aluminium bench allow vertical focussing. Beam size adjustment and instrumental background optimization is achieved with several sets of slits.

(d) Variable focussing. Due to the limited active size and resolution of the detectors and the wide scattering range of the samples (the samples under investigation scatter from $(0.4 \text{ nm})^{-1}$ to more than $(50 \text{ nm})^{-1}$), the focus has to be variable from about 0.3 m to 6 m behind the samples. At the so-called small-angle scattering beamlines of EMBL (X13 and X33, respectively) this is achieved by a bendable monochromator and a set of plane quartz mirrors aligned on an aluminium bench which is bent as a whole. With the exception of the Laue crystallographic experiments all time-resolved experiments at EMBL have been performed on beamlines X13 or X33, respectively. They are described in Refs. [12, 13].

(e) Remote control. About 30 stepping motors for beamline optimization and sample adjustment and manipulation have to be remotely controlled.

For most diffraction experiments on biological samples a narrow band pass is not necessary. Since both small and large samples are used, a long mirror is necessary for a high flux beamline in order to accept the full divergence of the beam. The mirrors serve both for focussing and harmonic rejection. In Fig. 2 the X13 beamline is sketched.

3. Detectors

The variety of samples and experiments requires special detectors for individual applications. This what was said on beamline requirements is also true for detectors. The optimal detector should have a high spatial resolution (200 μm) in two dimensions, high local (5×10^5 counts/s) and total count (5×10^7 counts/s) rates, a dynamic range of 10^4 , no noise, high sensitivity, energy resolution because of harmonic components in the beam, large active size of 200 mm \times 200 mm, long term stability, a time resolution of 10 μs or less and easy to use.

This "ideal" detector is obviously not to be realized as a single system. For a variety of applications in biology a 120 mm long one-dimensional detector with a spatial resolution of about 0.6–1 mm is sufficient. The current limitations in the experiments described below lie on the local and total count rate capabilities and the read-out times of the data in the memory. At EMBL, we routinely use photon counting gas-filled detectors of the delay-line type [14] or multiwire proportional chambers with count rates up to 20 MHz and a spatial resolution of 1 mm [15]. For lower time resolution, CCD, TV-type or diode-array detectors offer the advantage of better spatial resolution even in two dimensions (see e.g. [1]). Integrating detectors like storage phosphors [16] are not routinely used yet.

4. Trigger mechanisms

In order to investigate changes in a sample, one needs some appropriate means for initiation. This is in principle possible by any method which is fast compared to the processes under investigation. Examples used so far are rapid mixing to induce pH changes for studying the assembly kinetics of brome mosaic virus capsids [17] or ionic strength changes inducing actin polymerization [18]. Further possibilities are electric field pulses to orient tobacco mosaic virus [19].

One of the first millisecond time-resolved experiments have been performed to elucidate molecular mechanisms in muscle contraction using electrical stimulation of isolated living muscle fibres incubated in oxygenated Ringer solution (see e.g. [20] or for review [21]). More recently, Cecchi et al. [22] extended this approach to work on single muscle fibres only 100 μm in diameter.

In a large variety of time-resolved measurements, changes in temperature (T-jump) were used to initiate structural or conformational changes. Various methods were used so far:

(i) Change via heat conduction. The major advantage is the ability to vary the temperature both in cooling and heating direction. Using e.g. 4 water baths

set at different temperatures, Renner et al. [23] achieved T-jumps of 37° within a half-time of 2 s. Lipid phase transitions have been studied with this technique [24].

(ii) Joule heating. By discharging a high-voltage capacitor bank over the sample, homogeneous T-jumps of 5° within a few microseconds are feasible. Since the sample has to be electrically conductive, it requires often high salt concentrations. This method is hardly used in time-resolved X-ray experiments.

(iii) Heating by absorption of electromagnetic radiation. Fast and large amplitude T-jumps are possible. To avoid thermal gradients within the sample, care has to be taken in the selection of the proper wavelength. Water has strong absorption bands in the infrared. Laser heating is especially useful for biological samples since they are usually in an aqueous environment. On absorbing a photon in the near infrared, a vibrational mode is excited which relaxes thermally within 150 ps. Aspects and selection criteria for a T-jump laser are discussed in Ref. [25] and summarized in Fig. 3 and Table, respectively. For X-ray experiments, where the

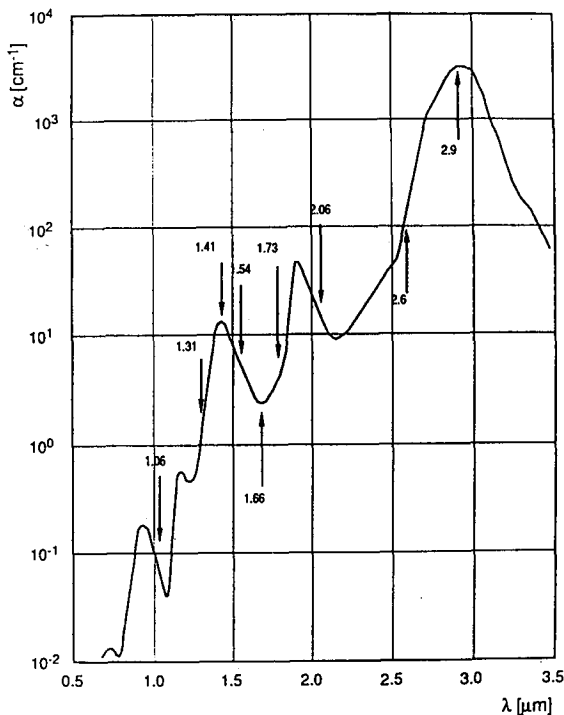


Fig. 3. Absorption spectrum of water in the near infrared. Some laser lines are shown. See also Table.

optimal thickness of biological samples is about 1 mm, the erbium-glass laser is a suitable tool. It is a versatile system, T-jumps of up to 20° within 2 ms or up to 2° within less than 1 μs have been achieved.

TABLE

Some aspects which have to be considered for laser T-jump experiments. Abbreviations: l — wavelength, α — linear absorption coefficient of water at the respective wavelength, I_0/e — absorption length, i.e. pathlength where the input energy decayed to I_0/e , E — laser pulse energy necessary for $dT = 5^\circ$ in $25 \mu\text{l H}_2\text{O}$ in a $5 \times 5 \text{ mm}^2$ cuvette with 1 mm path length.

Laser	l [μm]	α [cm^{-1}]	I_0/e [mm]	E [J]
Ruby	0.69	~ 0.01	~ 1000	~ 500
Nd:YAG	1.06	~ 0.1	~ 100	~ 50
I_2	1.31	~ 1.5	~ 6.6	~ 3.6
N_2 Raman	1.41	~ 11	~ 0.9	~ 0.75
Er:glass	1.54	6.5	1.5	1.05
Er:YAlO ₃	1.66	~ 4	~ 2.5	~ 1.5
Er:YLF	1.73	~ 5	~ 2	~ 1.3
Ho:YLF	2.07	37	0.27	0.5
Er:YAlO ₃	2.92	~ 5000	~ 0.002	—

Using microwaves Caffrey et al. [26] heated their samples by about $30^\circ/\text{s}$. This technique requires expensive and sophisticated temperature monitoring equipment.

Changing the chemical composition within the sample rapidly and homogeneously found a variety of applications. The technique became possible with the synthesis of so-called caged-compounds ([27], for review see also [28]). These are photolabile but metabolically inert derivatives of nucleotides or chelators of e.g. Ca^{2+} (Fig. 4). These compounds are allowed to diffuse into the sample, after which photolysis with a powerful flash of UV light releases the metabolically active substance. Flash photolysis of caged-compounds is widely used in physiological experiments. Examples are given in the following sections and reported by Blaisie et al. [30].

Excitation by direct absorption of light is a further possibility as will be described in the section on bacteriorhodopsin.

5. Experiments on muscle contraction

Experiments on muscle contraction played an important role in the development of strategies and instrumentation in synchrotron X-ray diffraction. Therefore it is justified to give a quick glance on historical aspects.

It was known since the sixties that the X-ray diffraction pattern of muscle shows marked differences depending on the physiological state of muscle, i.e.

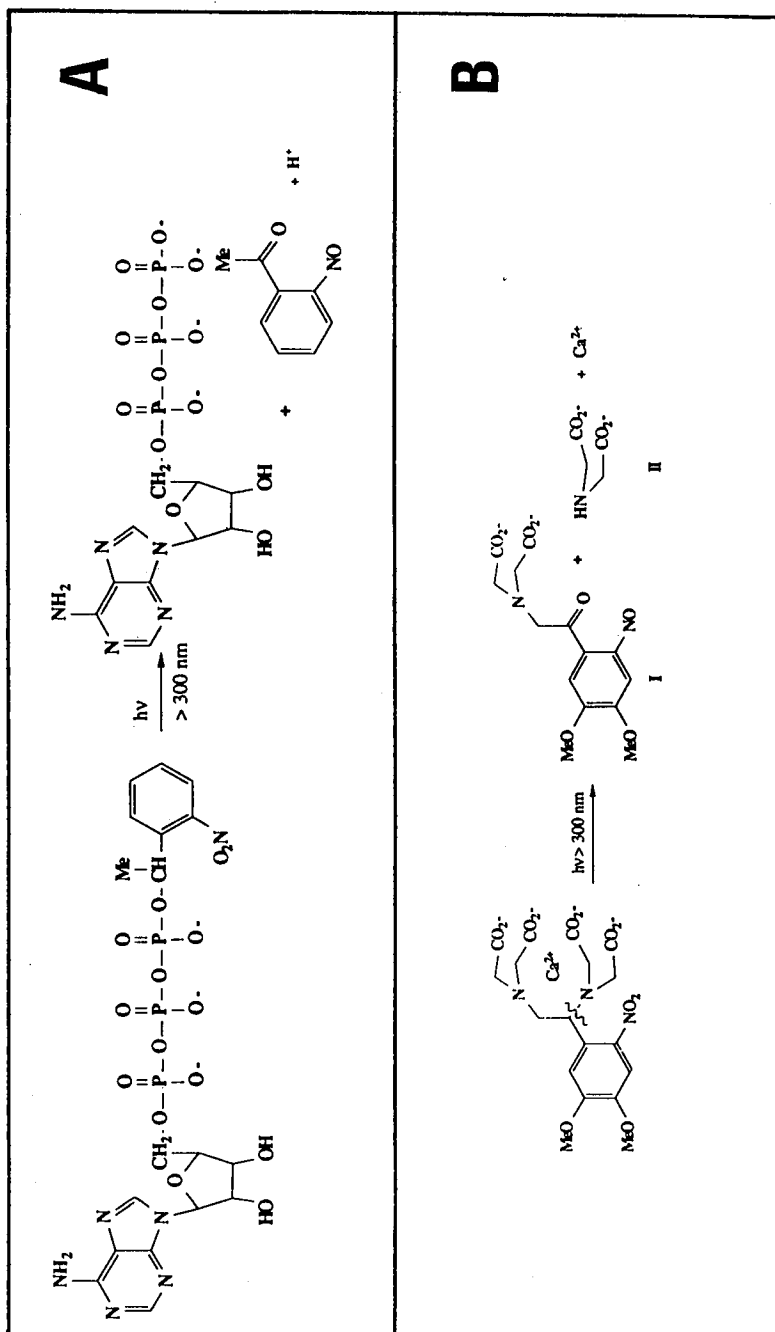


Fig. 4. Caged-ATP (A) and caged-Ca²⁺ (B) (after Kaplan and Ellis-Davies [29]).

whether it is relaxed, active or in the rigor mortis state [31, 32]. It was a fascinating idea to follow structural changes on the molecular level in real time using X-ray diffraction. Since DESY in Hamburg was one of the only synchrotrons operating at high enough energy for X-rays at that time, Prof. Holmes and co-workers set up there the first X-ray diffraction beamline which was intended to be used in the field of muscle contraction. First results of this effort were shown by Rosenbaum, Holmes and Witz [33]. However, this was only the first step towards real-time experiments, but nevertheless with synchrotron X-ray diffraction, data collection times on films could be reduced from up to several days (the strongest reflections in muscle have a scattering power of about 10^{-6}) to hours or minutes (see [34]). At about that time Gabriel and Dupont [35] developed a position sensitive electronic detector, another major requirement for time-resolved experiments. But not until the end of the seventies, the first real-time X-ray experiments on muscle using a two-dimensional TV detector became feasible [20].

The experimental approach to visualize structural changes on the molecular level during muscle contraction is briefly outlined in the following.

Skeletal muscle fibres are about $100\ \mu\text{m}$ in diameter and up to several cm in length. The basic contractile unit is the sarcomere which consists of an array of interdigitating filamentous aggregates of actin and myosin (Fig. 5a). Cyclic in-

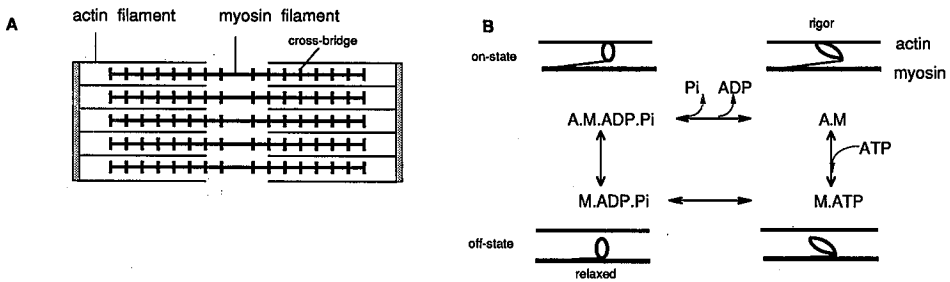


Fig. 5. (a) The sarcomere is the basic contractile unit of a muscle fibre. It consists of interdigitating sets of myosin and actin filaments which slide past each other during muscle contraction. (b) relation between biochemical and structural states of muscle fibres. In the rigor state actin (A) and myosin cross-bridges (M) are tightly bound (A.M.). Adding ATP causes this complex to dissociate (M.ATP). After hydrolysis of ATP to ADP and inorganic phosphate (Pi) the muscle is relaxed (M.ADP.Pi). Rebinding of M.ADP.Pi to actin (A.M.ADP.Pi) and release of Pi and ADP leads to tension production and closing the cycle. Movement of the cross-bridges is seen in the X-ray diffraction pattern (after [25]).

teractions of so-called cross-bridges (radial projections of the myosin filaments) with actin cause the filaments to slide past each other during muscle shortening. The energy necessary for muscle (and most other energy consuming processes in living systems) is supplied via adenosine-triphosphate (ATP). From kinetic experiments on isolated muscle proteins in solution, a scheme was established which correlates biochemical states with structural ones. A simplified model is shown

in Fig. 5b. For review see Refs. [36, 37]. In rigor, the energetically lowest state, myosin cross-bridges and actin are strongly bound. Addition of ATP causes this complex to dissociate with subsequent hydrolysis of ATP to adenosine-diphosphate (ADP) and phosphate. If regulatory proteins in the actin filament switch it in the "on-state", the cross-bridges can rebind to actin and produce tension after release of phosphate and ADP. Although the reactions are reversible, there is a net flux in the clockwise direction.

The X-ray pattern of muscle fibres is divided into equatorial, meridional, and layer line reflections. The first ones arise from the hexagonal arrangement (in the cross-section) of myosin and actin filaments (see Fig. 5a), the meridional ones are attributed to longitudinal periodicities of the filaments and the layer lines arise from helical structures within the filament. For example, in rabbit psoas muscle, the two strongest reflections are the equatorial 10 and 11 reflections. The 10 reflection arises from Bragg planes consisting only of the myosin filament whereas the 11 reflection originates from planes including both myosin and actin filaments. Depending on the physiological state of the muscle, the cross-bridges are located closer to one or the other filament. This is clearly seen in the X-ray pattern. In relaxed muscle the 10 reflection is stronger than the 11 and vice versa in activated or rigor muscle (see Fig. 5b). Similar changes in other reflections occur if e.g. longitudinal or helical order on the filaments increases or decreases in a given physiological state.

The first time-resolved experiments are based on the discovery of Galvani and Volta more than 200 years ago that isolated frog muscle fibres contract upon an electrical stimulus. In this approach the muscle is kept in physiological salt solution where it can survive for days and is electrically stimulated. The X-ray reflections are recorded simultaneously with mechanical signals like tension and stiffness. From these data and the comparison of their time courses, a detailed picture of structural changes during muscle contraction was depicted in recent years. For references see e.g. [21, 22].

To manipulate the chemical composition inside the muscle cell in analogy to those experiments on isolated proteins in solution, skinned fibres, i.e. muscle fibres whose cell membrane has been removed or rendered permeable, are often used. This treatment retains all of the contractile properties of living muscle fibres except for the response to electrical stimulation.

The aim of these experiments is to model and fit kinetic constants obtained from experiments on muscle fibres and to compare them with those obtained on isolated muscle proteins in solution. In the latter experiments, the tension producing step is missing and therefore rate constants of one or more steps in the kinetic scheme should be different. From the differences it should be possible to pin-point the tension generating step in the cross-bridge cycle.

The experimental approach is to rapidly vary the chemical composition using caged-compounds or to change the temperature in the fibres. The effects of these changes can be studied at e.g. different mechanical loads of the fibres.

An example of this approach is shown in Fig. 6. In the absence of ATP the fibres are trapped in the rigor conformation with the cross-bridges in the vicinity of the actin filament giving strong 11 and weaker 10 reflections. Rapid release of ATP

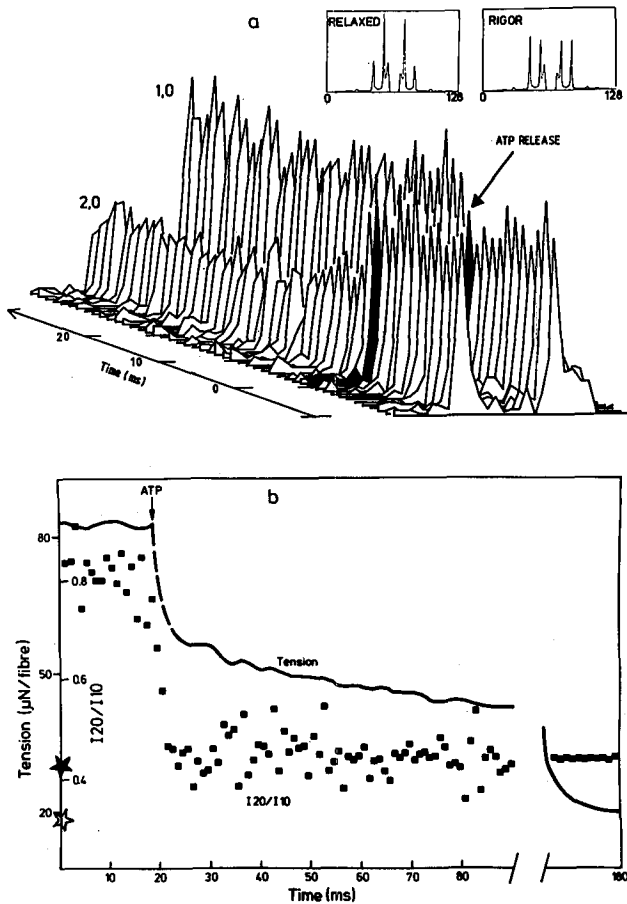


Fig. 6. (A) Three-dimensional representation of equatorial diffraction patterns at a time-resolved study of the relaxation process in insect muscle fibres. In rigor, the 20 reflection is strong and the 10 is weaker and vice versa in relaxed muscle. (B) Comparison of the time courses of the ratio of the integrated intensities and the tension relaxation after photolytic release of ATP.

from caged-ATP (Fig. 4a) allows us to measure the time course of the dissociation of the cross-bridges from actin. For details of this approach see Refs. [38, 39].

The results showed that (i) ATP binding and cross-bridge dissociation in muscle fibres is as fast as in solution and is not strain sensitive, (ii) the strain sensitive step must come before ADP release, (iii) the changes in the equatorial reflections lead the tension signal both in the activation and relaxation direction.

6. Non-equilibrium phase transitions in phospholipids

Phospholipids are the major constituents of cell membranes. They exist in a variety of phases depending on thermodynamic variables. According to their sym-

metries, lipid structures are characterised as one-dimensional lamellar, two-dimensional hexagonal and three-dimensional cubic. For review see Refs. [40, 41]. The mechanisms accompanying their interconversions are hitherto unknown. They are widely investigated for understanding membrane structure and function and are discussed in the framework of statistical mechanics and non-equilibrium thermodynamics [42, 43]. Time-resolved experiments on lipid phase transitions are reviewed in e.g. [44, 45].

The simplest case of a symmetry conserving lamellar-lamellar transition of dimyristoyl-phosphatidyl-ethanolamine (DMPE) is shown in Fig. 7. Below 49.5°C and under fully hydrated conditions it exists in the L_β or gel phase where the aliphatic chains are aligned. In the small-angle region, the X-ray pattern shows reflections of a one-dimensional lattice with about 5.2 nm lattice spacing. In the wide-angle part, a further reflection is seen at about $(0.43 \text{ nm})^{-1}$. Melting of the aliphatic chains causes the lattice to shrink to 4.3 nm and the wide-angle reflection to disappear. The following questions arise: (i) what is the time course of the transition, (ii) how does it depend on the driving force, i.e. the final temperature after the jump, (iii) do the small- and wide-angle reflections change on the same time scale, and (iv) what are the transition pathways, are there disordered intermediates?

To answer these questions, two delay-line type detectors have been electronically connected in series, one of them covered the wide-angle region, the other the small-angle region. Temperature jumps of durations of less than 1 μs and 2 ms with amplitudes from 2° to 15° have been applied. In the example shown, diffraction patterns have been collected with 2 ms time resolution. On this time scale both wide- and small-angle reflections change with similar time courses. No disordered structures could be detected. The transition proceeds via two-state martensitic mechanisms involving concerted disclinations about lattice connected transition planes. For details see [46].

The aim in these experiments is manifold. In equilibrium or near equilibrium studies, synchrotron X-ray diffraction allows determination of phase diagrams similar to experiments on stationary sourced but in much shorter exposure times. Thermodynamically, there is a linear relationship between driving forces and fluxes. This linearity can be lost at larger deviations from equilibrium and qualitative changes can occur. Using the laser T-jump approach, this effect was indeed seen in transitions in phospholipids from the lamellar to the inverse hexagonal phase. Short-lived intermediate structures appeared which are not seen in X-ray diffraction experiments under near equilibrium conditions. It has been shown that the systems respond to the high thermodynamic driving forces by forming correlated intermediate structures which provide efficient pathways for relaxation [46].

At the EMBL beamline X33, experiments of this type have been performed with up to 100 μs time resolution while the signal-to-noise ratio is still excellent.

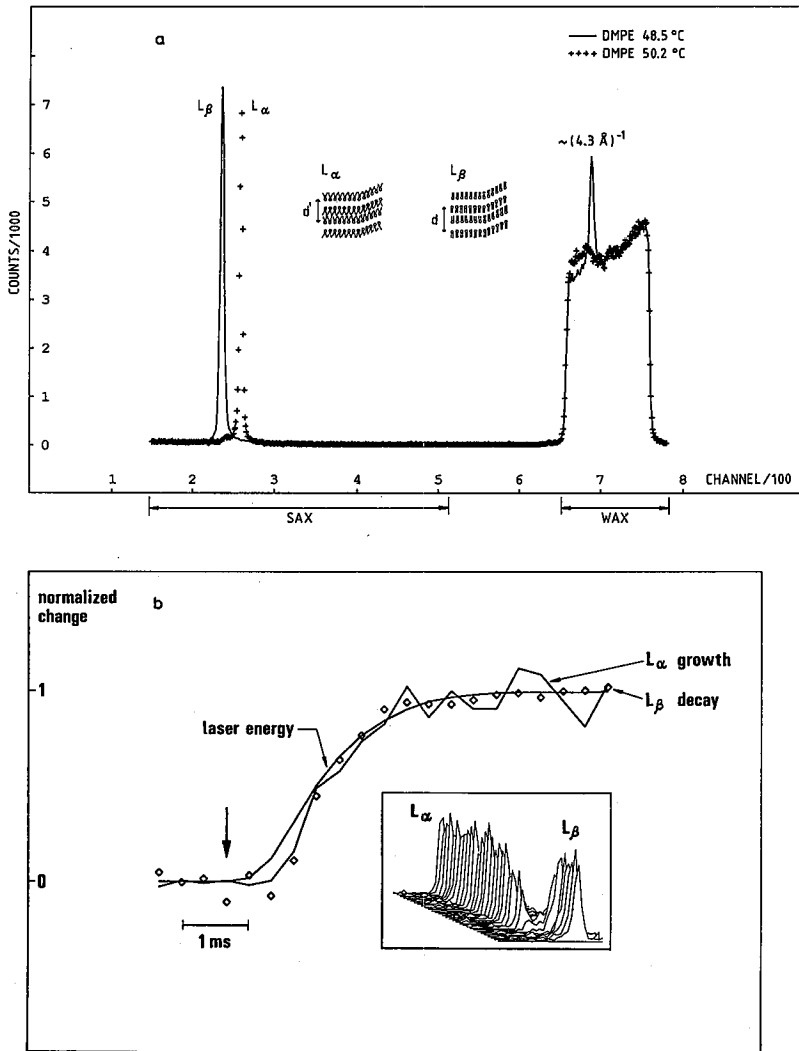


Fig. 7. (A) Superimposed diffraction pattern of DMPE in the gel (L_β) and liquid crystalline (L_α) phase. Two linear delay-line detectors in series cover the small-angle (SAX) and the wide-angle (WAX) region. (B) Time course of the first-order reflections after a T-jump with $350 \mu\text{s}$ time resolution. The structural changes occur as rapidly as the heating of the sample.

7. Flash excitation studies on bacteriorhodopsin

Bacteriorhodopsin (BR), an integral membrane protein found in the purple membranes of halophilic bacteria, pumps proton out of the cell by direct utilization of light. See e.g. [47, 48]. Upon absorption of a photon by the chromophore retinal, BR passes through a series of spectroscopically well-characterized states (Fig. 8a).

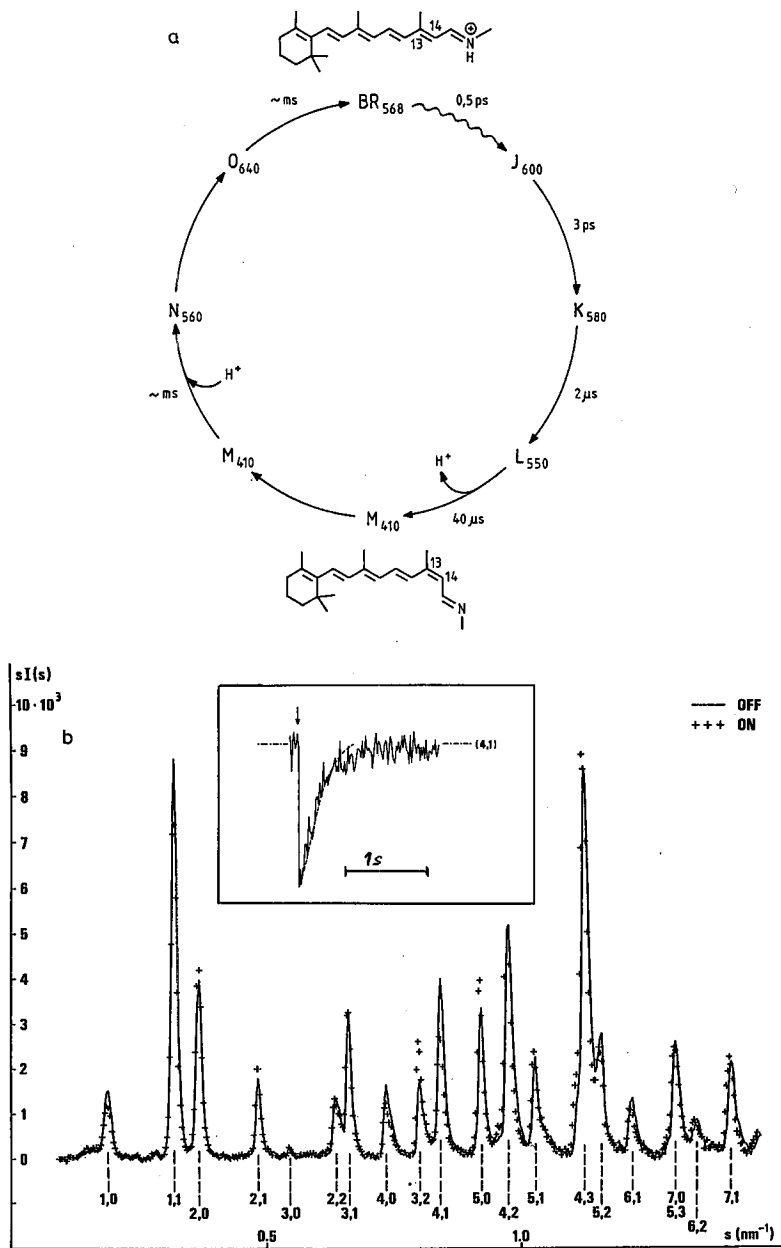


Fig. 8. (A) The photocycle of bacteriorhodopsin. In the ground state absorption is maximal at 568 nm. After absorbing a photon, it passes through a series of spectroscopically characterized states. During this cycle, a proton is released to the outside of the cell followed by a proton uptake inside the cell. (B) Diffraction pattern of BR with and without illumination. Reflections are indexed on a hexagonal lattice. The inlay shows the time course of the 41 reflection after a flash. The time resolution is 15 ms.

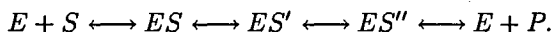
Conformational differences between the ground state and the M-intermediate have been detected by neutron diffraction [49].

Using synchrotron X-ray diffraction we have been able to reproduce these findings. In a first attempt, we used a powerful flash lamp [50] and measured the diffraction pattern after flash excitation with 15 ms time resolution [7]. Figure 8b shows the diffraction pattern of BR in the ground state and under continuous illumination. Intensity changes in both increasing and decreasing directions are clearly seen in various reflections. After flash excitation the intensity changes of the reflections proceed with similar time courses and in parallel with the decay of the spectroscopic M-intermediate as measured via absorption changes at 410 nm. The experiments show that the chromophore retinal induces an overall conformational change in the protein which relaxes to its ground state after uptake of a proton. The ultimate aim of this experiment would be to calculate the electron density distribution during the photocycle.

For a more detailed analysis of this process it is necessary to record more spectroscopic information simultaneously with the X-ray data. Experiments of this type are in progress. Using a diode-array spectrophotometer covering the range from 350 nm to 700 nm with a 700 μ s read-out time, a much more detailed correlation of structural and spectroscopic data should be possible.

8. Time-resolved macromolecular crystallography

Most of the structures of macromolecules solved to high resolution are enzymes, either as the free enzyme or as a complex with a substrate, product or co-factor. The kinetic scheme of enzyme catalysis is generally described as follows:



The enzyme E and the substrate S make an enzyme-substrate complex ES which, after one or more intermediate complexes ES' , dissociates leaving the enzyme and the product. An example is hexokinase which catalyses phosphoryl transfer from adenosine-triphosphate (ATP) to glucose, leaving adenosine-diphosphate (ADP) and glucose-6-phosphate.

With X-ray crystallography, the structures of a few hundred enzymes have been determined to atomic resolution. However, fully understanding the complete function of an enzyme requires knowledge of the structures of the free enzyme and of all the intermediate complexes. In this respect, time-resolved macromolecular crystallography is a promising thought to determine the three-dimensional structures of intermediates occurring during the reaction. See e.g. [51-53] and references therein. However, experimental and theoretical limitations prevented this method from becoming a routine tool. For example, the life times of enzyme-substrate intermediate complexes are as short as nanoseconds, protein crystals are difficult to grow and usually available only in small quantities. Some of the limitations can be overcome by e.g. cooling, which slows down the rate constants.

Standard Bragg diffraction takes too long to record a data set of even the slowest reactions. Here Laue diffraction offers a promising alternative. Under ideal circumstances one could obtain an almost complete data set within one exposure.

The current problems associated with this technique are:

(i) Its higher sensitivity to mosaicity as compared to Bragg diffraction. The diffraction spots lie close to each other and cannot be separated if the mosaicity is too high.

(ii) The temperature sensitivity of proteins. The wavelength band of a Laue beamline ranges from about 0.04 nm to 0.2 nm. With the high photon flux, problems arise due to heat absorption and dissipation.

(iii) Measurement of a given intermediate is only possible if this accumulates during the reaction.

(iv) Too large overall structural changes can lead to disordering. This was seen in well diffracting hexokinase crystals after diffusion of glucose into the crystal [53]. Within seconds the lattice was disordered and partially reannealed after about 3 min.

(v) The question has to be answered whether the enzymatic reaction in solution is similar to the one in the crystal.

In the final part, a Laue crystallographic study on the protein H-ras p21 is described in more detail. This protein with a molecular weight of 21000 Da is believed to be involved in signal transmission and cell proliferation. It is active when guanosine-triphosphate (GTP) is bound and inactive after hydrolysis, when guanosine-diphosphate (GDP) is bound. It is stable only with a bound nucleotide. By nature of its enzymatic activity, crystals cannot be grown as p21.GTP complexes, since GTP would be hydrolyzed with a half-life of 40 min at 20°C to GDP. However, it was possible to grow crystals of caged-GTP.p21 complexes. After photolytic release of GTP from caged-GTP within the crystal, it was found that the kinetics of hydrolysis is the same as in solution [54]. In a Laue crystallographic study using p21 complexes with caged-GTP, the structures of the complexes before photolysis, i.e. with caged-GTP, 2 minutes after photolysis and 14 minutes later have been solved in one single crystal [55]. Substantial structural differences have been found before and after GTP hydrolysis. From this study it is evident that there are many interactions between the phosphate groups, the protein and Mg^{2+} which changes its coordination during the reaction.

The aforementioned problems associated with Laue crystallography of proteins have not been too severe in these experiments with p21 since (i) the reaction is slow enough, allowing longer exposures with reduced photon flux and heat load and (ii) the overall conformational change is small compared to e.g. hexokinase.

9. Summary

The presented experiments should serve as examples to show how synchrotron radiation X-ray diffraction can be used in "imaging" conformational or structural changes down to the molecular level in biological samples during their action. The approach of time-resolved X-ray diffraction aims to bridge structural and functional aspects. The new generation of synchrotron facilities with much higher brilliance will certainly enable experiments with better time resolution, especially on smaller samples. To take full advantage of the new sources, developments of the detector site have to be forced too.

Acknowledgement

Most of the experiments described in more detail have been carried out as collaborations with other colleagues. In particular we gratefully acknowledge the collaboration with Drs. R. Goody, Y. Maeda, K. Poole and J. Wray in experiments on muscle contraction; G. Büldt, N. Dencher and M. Koch on flash excitation studies on bacteriorhodopsin; M. Koch, M. Kriechbaum and P. Laggner on lipid phase transitions; and R. Goody and I. Schlichting on the p21 Laue crystallography experiments.

References

- [1] S.M. Gruner, *Science* **238**, 305 (1987).
- [2] *Uses of Synchrotron Radiation in Biology*, Ed. H.B. Sturmann, Academic Press, London 1982.
- [3] *Structural Biological Applications of X-Ray Absorption, Scattering and Diffraction*, Eds. H.D. Bartunik, B. Chance, Academic Press, London 1986.
- [4] *Synchrotron Radiation in Chemistry and Biology I. Topics in Current Chemistry*, Vol. 145, Ed. E. Mandelkow, Springer, Berlin 1988.
- [5] *Synchrotron Radiation in Chemistry and Biology II. Topics in Current Chemistry*, Vol. 147, Ed. E. Mandelkow, Springer, Berlin 1988.
- [6] *Handbook on Synchrotron Radiation*, Vol. 4, Eds. S. Ebashi, M.H.J. Koch, E. Rubenstein, North-Holland, Amsterdam 1991.
- [7] M.H.J. Koch, in Ref. [6], p. 243; M.H.J. Koch, Dencher, D. Oesterhelt, H.-J. Plöhn, G. Rapp, G. Büldt, *EMBO J.* **10**, 521 (1991).
- [8] P. Fratzl, *Acta Phys. Pol. A* **82**, 121 (1992).
- [9] R. Haensel, *Acta Phys. Pol. A* **82**, 33 (1992).
- [10] Å. Kvick, *Acta Phys. Pol. A* **82**, 7 (1992).
- [11] C. Malgrange, *Acta Phys. Pol. A* **82**, 13 (1992).
- [12] J. Hendrix, M.H.J. Koch, J. Bordas, *J. Appl. Crystallogr.* **12**, 467 (1979).
- [13] M.H.J. Koch, J. Bordas, *Nucl. Instrum. Methods Phys. Res. A* **208**, 461 (1983).
- [14] A. Gabriel, *Rev. Sci. Instrum.* **48**, 1303 (1977).
- [15] J. Hendrix, H. Fürst, B. Hartfield, D. Dainton, *Nucl. Instrum. Methods* **201**, 139 (1982).

- [16] J. Miyahara, K. Takahashi, Y. Amemiya, N. Kamiyaha, Y. Satow, *Nucl. Instrum. Methods Phys. Res. A* **246**, 572 (1986).
- [17] C. Berthet-Colominas, M. Cuillel, M.H.J. Koch, P. Vachette, B. Jacrot, *Eur. Biophys. J.* **15**, 159 (1987).
- [18] Z. Sayers, M.H.J. Koch, J. Bordas, U. Lindberg, *Eur. Biophys. J.* **13**, 99 (1985).
- [19] M.H.J. Koch, E. Dorrington, R. Kläring, A.M. Michon, Z. Sayers, R. Merquet, C. Houssier, *Science* **240**, 194 (1988).
- [20] H.E. Huxley, A.R. Fauqi, J. Bordas, M.H.J. Koch, J.R. Milch, *Nature* **284**, 140 (1980).
- [21] H.E. Huxley, A.R. Faruqi, *Ann. Rev. Biophys. Bioeng.* **12**, 381 (1983).
- [22] G. Cecchi, A.M. Bagni, P.J. Griffiths, C.C. Ashley, Y. Maeda, *Science* **250**, 1409 (1990).
- [23] W. Renner, E.-M. Mandelkow, E. Mandelkow, J. Bordas, *Nucl. Instrum. Methods* **208**, 535 (1983).
- [24] P. Laggner, in: *Topics in Current Chem.*, Vol. 147, Ed. E. Mandelkow, Springer, Heidelberg 1988, p. 173.
- [25] G. Rapp, R.S. Goody, *J. Appl. Crystallogr.* **24**, 857 (1991).
- [26] M. Caffrey, G. Fanger, R.L. Magin, J. Zhang, *Biophys. J.* **58**, 677 (1990).
- [27] J.H. Kaplan, B. Forbush III, J. Hoffman, *Biochem.* **17**, 1929 (1978).
- [28] J.A. McCray, D.R. Trentham, *Ann. Rev. Biophys. Biophys. Chem.* **18**, 239 (1989).
- [29] J.H. Kaplan, G.C.R. Ellis-Davies, *Proc. Natl. Acad. Sci. USA* **85**, 6571 (1988).
- [30] J.K. Blaisie, L.G. Herbette, D. Pascolini, V. Skita, D.H. Pierce, A. Scarpa, *Biophys. J.* **48**, 9 (1985).
- [31] M.K. Reedy, K.C. Holmes, R.T. Tregear, *Nature* **207**, 1276 (1965).
- [32] H.E. Huxley, G. Brown, *J. Mol. Biol.* **30**, 383 (1967).
- [33] G. Rosenbaum, K.C. Holmes, J. Witz, *Nature* **230**, 129 (1971).
- [34] R.S. Goody, K.C. Holmes, H.G. Mannherz, J. Barrington-Leigh, G. Rosenbaum, *Biophys. J.* **15**, 687 (1975).
- [35] A. Gabriel, Y. Dupont, *Rev. Sci. Instrum.* **43**, 1601 (1972).
- [36] A. Taylor, *Crit. Rev. Biochem.* **6**, 103 (1979).
- [37] M.A. Geeves, R.S. Goody, H. Gutfreund, *J. Musc. Res. Cell Mot.* **5**, 351 (1984).
- [38] G. Rapp, K.J.V. Poole, Y. Maeda, K. Güth, J. Henrix, R.S. Goody, *Biophys. J.* **50**, 993 (1986).
- [39] K.J.V. Poole, Y. Maeda, G. Rapp, R.S. Goody, in: *Adv. Biophys.*, Vol. 27, Ed. M. Kotani, Elsevier, Limerick 1991, p. 63.
- [40] *Handbook of Lipid Research*, Vol. 4, Ed. D.A. Small, Plenum Press, London 1986.
- [41] G. Cevc, D. Marsh, *Phospholipid Bilayers*, Wiley, New York 1987.
- [42] H. Haken, *Synergetics. An Introduction*, Springer, Berlin 1983.
- [43] L.D. Landau, E.M. Lifshitz, *Course of Theoretical Physics*, Vol. V, Pergamon Press, New York 1980.
- [44] M. Caffrey, *Ann. Rev. Biophys. Chem.* **18**, 159 (1989).
- [45] P. Laggner, M. Kriechbaum, *Chem. Phys. Lipids* **57**, 121 (1991).
- [46] P. Laggner, M. Kriechbaum, G. Rapp, *J. Appl. Crystallogr.* **24**, 836 (1991).

- [47] W. Stoeckenius, R.A. Bogomolni, *Ann. Rev Biochem.* **52**, 587 (1982).
- [48] R. Henderson, J.M. Baldwin, T.A. Ceska, F. Zemlin, E. Beckmann, K.H. Downing, *J. Mol. Biol.* **213**, 899 (1990).
- [49] N.A. Dencher, D. Dresselhaus, G. Zaccai, G. Büldt, *Proc. Natl. Acad. Sci. USA* **86**, 7876 (1989).
- [50] G. Rapp, K. Güth, *Pflügers Arch.* **411**, 200 (1988).
- [51] K. Moffat, *Ann. Rev. Biophys. Biophys. Chem.* **18**, 309 (1989).
- [52] J. Hajdu, in: *2nd Europ. Conf. Prog. X-Ray Synchrotron Radiat. Res., Conf. Proc.*, Vol. 25, Eds. A. Balerna, E. Bernieri, S. Mobilio, SIF, Bologna 1990.
- [53] H.D. Bartunik, in Ref. [6], p. 147.
- [54] I. Schlichting, G. Rapp, J. John, A. Wittinghofer, E. Pai, R.S. Goody, *Proc. Natl. Acad. Sci. USA* **86**, 7687 (1989).
- [55] I. Schlichting, S.C. Almo, G. Rapp, K. Wilson, K. Petratos, A. Lenfer, A. Wittinghofer, W. Kabsch, E. Pai, G.A. Petsko, R.S. Goody, *Nature* **345**, 309 (1990).